Journal of Electroceramics, 11, 191–206, 2003

Defect Chemistry and Charge Transport in $SrBi_2Nb_2O_9$

A.C. PALANDUZ* & D.M. SMYTH†
Materials Research Center, Lehigh University, 5 E. Packer Ave. Bethlehem, PA 18015, USA

Submitted July 1, 2003; Revised January 20, 2004; Accepted January 22, 2004

Abstract. Equilibrium dc conductivity and thermopower measurements at 650–800°C on undoped and 1% acceptor-doped $SrBi_2Nb_2O_9$, SBN, indicate that the *n*-type conductivity is similar to that of a simple transition metal oxide that contains 1–2% donor excess. The donor content is attributed to the presence of Bi^{+3} on Sr^{+2} sites in the perovskite-like layers of the structure. These centers arise from cation place exchange between these ions in the alternating layers of the crystal. This exchange is apparently not completely self-compensating, and there is local charge compensation in each layer. While the equilibrium conductivity of $SrBi_2Ta_2O_9$, SBT, is dominated by ionic conduction in the Bi layers, in SBN conduction by electrons in the perovskite-like layers prevails. The difference in behavior is attributed to the expected smaller band gap of the niobate. The electron mobility in SBN is extremely small, of the order of 10^{-5} $cm^2/v \cdot sec$ at 750°C, and is highly activated with an activation energy of about 1.6 eV. The resulting low mobility at ambient temperatures is proposed as the basis for the observed resistance to ferroelectric fatigue. Reports of metallic Bi on the surface of SBT and SBN by XPS analysis are shown to result from the highly reducing atmosphere of the XPS apparatus.

Keywords: SBN, defect chemistry, seebeck, ferroelectric fatigue, conductivity

Introduction

The use of ferroelectric thin films as memory elements on computer chips is being actively studied and, in some cases, has reached the marketplace. The memory is stored as the polarization direction which can be switched by the application of a dc field. For some ferroelectrics, such as the PZT-based materials, the amount of switchable charge may degrade after 10^6–10^8 switching cycles. This can reach the point that the polarization direction can no longer be determined, a phenomenon known as ferroelectric fatigue. On the other hand, the Bi-layer ferroelectrics, or Aurivillius phases, have been found to be highly resistant to fatigue [1]. These compounds have layered structures, with Bi-containing layers alternating with perovskite-like layers. The favored composition so far for memory elements is $SrBi_2M_2O_9$, with M = Ta or Nb. It has been shown that defects play an important role in ferroelectric fatigue [2–5], so it is of interest to determine what aspects of the defect chemistry of these compounds contribute to their stability.

In the compounds $SrBi_2Ta_2O_9$ (SBT) and $SrBi_2Nb_2O_9$ (SBN), $Bi_2O_2^{+2}$ layers with a fluorite-like structure alternate with $SrM_2O_7^{-2}$ layers having a perovskite-like structure. Detailed structural studies have shown that there is extensive cation place exchange between the Bi^{+3} and Sr^{+2} sites [6, 7]. This exchange, which is of the order of several percent, results in the presence of Sr'_{Bi} acceptor centers in the Bi-layer, and $Bi^{\cdot}_{Sr}$ donor centers in the perovskite-like layers. In an isotropic structure such place exchange should be self-compensating, and no other defects would be required for charge balance. However, we have previously proposed that self-compensation is not wholly effective in these layered structures, and that there is a significant amount of charge compensation within each layer [8, 9]. Thus Sr'_{Bi} acceptor centers in the Bi layer can be partially

*Current address: Intel Corp., 5000 W. Chandler Blvd., CH5-159, Chandler AZ 85226-3699, USA.
†To whom all correspondence should be addressed. E-mail: dms4@lehigh.edu

compensated by oxygen vacancies, $V_O^{\cdot\cdot}$, or holes, $h^{\cdot}$, while the $Bi_{Sr}^{\cdot}$ donor centers in the perovskite layers can be partially compensated by cation vacancies, V_{Sr}'', or electrons, e'. The electrical conductivity in randomly oriented polycrystalline samples will then be dominated by the better conducting layer. In this model, each type of structural layer has a relatively independent defect chemistry. In an earlier study of the equilibrium electrical conductivity of SBT, we observed a broad plateau of ionic conductivity independent of the oxygen activity [9]. This was attributed to oxygen vacancy conduction in the Bi layers. This paper describes a similar study of SBN. The general chemical behavior of Ta^{+5} and Nb^{+5} is extremely similar, because they have the same ionic charge, and, because of the lanthanide contraction, almost identical ionic radii. In spite of this, and despite the isostructural nature of SBT and SBN, it will be seen that the defect chemistry of SBN is surprisingly different from that of SBT.

Experimental

SBN samples were prepared from appropriate amounts of $SrCO_3$, Bi_2O_3, and Nb_2O_5, using a modified version of Subbarao's technique [10]. SBN powders were calcined in a Pt crucible at 1050°C for one hour while embedded in calcined SBN packing powder in a double crucible arrangement. Phase identification was confirmed by X-ray diffraction using a Philips APD 1700 automated diffractometer with Cu Kα radiation.

High temperature equilibrium electrical conductivity measurements were made by the standard 4-point dc technique using Pt electrodes in a flowing gas stream composed of Ar-O_2 mixtures, or CO_2 depleted of oxygen by means of an electrochemical oxygen pump based on acceptor-doped ZrO_2. In order to minimize Bi_2O_3 loss during the conductivity measurements, a small amount of undoped SBN powder was placed under an alumina cover near the sample in order to provide a protective Bi_2O_3 atmosphere. The oxygen activity near the sample was measured with a yttria-doped zirconia sensor.

Constant composition oxygen activity measurements were made by equilibrating an undoped SBN sample in a small alumina cell that could be hermetically sealed with deformable glass gaskets [11]. The volume of enclosed gas was small enough so that the oxygen activity could be changed substantially without significant variation in the defect concentrations in the sample. The system was initially brought to equilibrium at 730°C and $\log P(O_2) = -1.8$ (atm.), and then sealed by exerting pressure on the softened glass gaskets. A stabilized zirconia lid served as a sensor to monitor the equilibrium oxygen activity as the temperature was varied between 730 and 670°C.

Thermoelectric power measurements were made by a heat pulse method, similar to that developed by Eklund and Mabatah [12]. A sintered, undoped SBN sample was equilibrated in a flowing Ar-O_2 mixture with $\log P(O_2) = -3.1$ (atm.) at 25° intervals in a temperature range between 650 and 800°C. An ac current was passed through a Pt heater wire at one end of the sample for 55–90 seconds, creating temperature differences between 53 and 80°C between the two ends. After the heater had been turned off for 15–20 seconds, thermopower data were collected for approximately 150 seconds. The large temperature difference allowed clear readings to be obtained in spite of the high electrical noise level observed in that range of oxygen activity. The thermoelectric emf and the thermocouple reading across the sample, which is proportional to the temperature difference, were measured as the gradient gradually diminished.

XPS measurements were performed with a Scienta ESCA-300 system using Al Kα radiation in order to monitor the state of bismuth on the surface of SBN and on a freshly-formed fracture surface created in the high vacuum chamber.

Experimental Results

The 4-probe, dc equilibrium electrical conductivity of undoped, polycrystalline SBN as a function of oxygen activity at temperatures between 700 and 775°C is shown in Fig. 1. The behavior is surprisingly different from that of SBT [9]. In the latter, there is a broad conductivity plateau, independent of oxygen activity, which proved to be ionic in nature. There were only slight upturns at the highest and lowest oxygen activities, which were attributed to hole conduction due to partial filling of oxygen vacancies at high activities, and to electron conduction due to loss of oxygen at low activities. Thus SBT is exhibiting classic acceptor-doped behavior, such as that seen in acceptor-doped zirconia or ceria. There are four different aspects to the behavior of SBN. In Region I, starting at 1 atm. and proceeding with decreasing oxygen activities, there is first

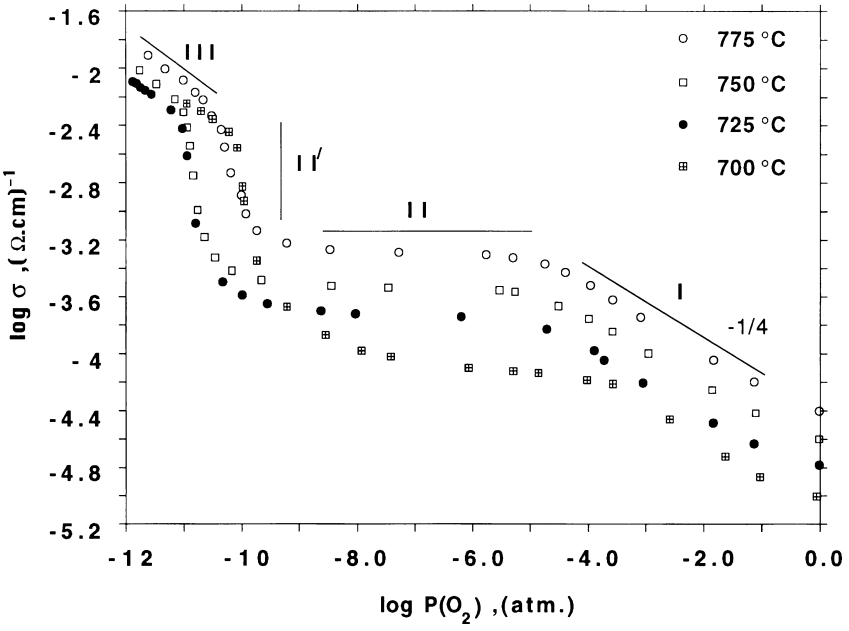

Fig. 1. The equilibrium conductivity curves for undoped SBN for values of temperature between 725°C and 775°C at 25°C intervals. The data points forming the conductivity "jump" are not equilibrium values, but were obtained during the transition, which typically lasted for about 8 hours for an isotherm.

a rising conductivity with a log-log slope of −1/4. This is followed by Region II, a flat plateau, that leads to an abrupt increase in conductivity, Region II′. There is finally a gradual increase in conductivity with a partially developed dependence on the oxygen activity, Region III. The measurements were checked for reproducibility and reversibility by periodic return to a reference condition, usually in pure oxygen. For oxygen activities lower than those for which data are shown in Fig. 1, the reference conductivities could not be reproduced, and this is believed to be caused by some kind of decomposition of the sample. These conditions were then avoided in subsequent measurements. Even when samples were held for extended times in the plateau region, near the abrupt rise in conductivity, similar evidence for irreversible change was observed. For that reason the data in Fig. 1 were obtained with minimal equilibration times in the region of low oxygen activity. These irreversibilities may be related to volatilization of Bi_2O_3. The electrical noise level in undoped SBN is high at high oxygen activities, although less than that observed in SBT [9]. The noise decreases with decreasing $P(O_2)$, until it virtually disappears at the abrupt conductivity rise.

The validity of the data shown in Fig. 1 must be addressed. Recent experimental results obtained by Ferreira et al. for 5 and 10% Nb-doped $SrTiO_3$ are qualitatively very similar to those shown in Fig. 1, including the abrupt jump in conductivity and the lower region of indeterminate slope [13]. However, those authors propose that both the plateau region and the abrupt jump are experimental artifacts related to the behavior of their oxygen activity sensor. They ignore the data in those regions and interpolate a linear connection between the regions of highest and lowest oxygen activities, Regions I and III. As a result of our experience with similar zirconia-based oxygen sensors over the past 30 years, we must respectfully disagree. Many different compounds have been studied and each was found to have its own characteristic and reproducible behavior over this central range of oxygen activities. The very different behavior of SBT and SBN is a good example. If the behavior were related to an experimental artifact, the nature of the sample should not matter. Thus we shall proceed with the supposition that the data as shown in Fig. 1 are a valid representation of the equilibrium conductivity of undoped SBN. Recent work on La-doped $SrTiO_3$ showed conductivity

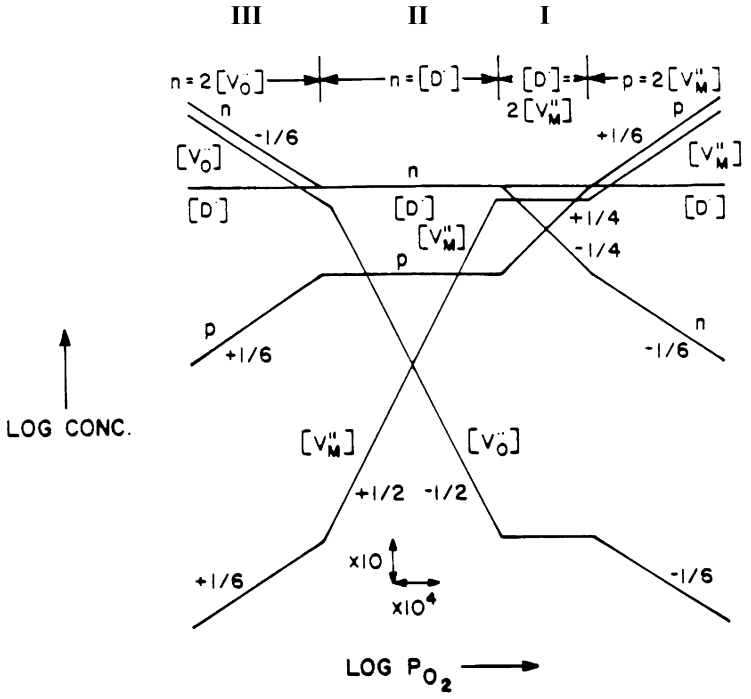

Fig. 2. Equilibrium defect diagram for a donor-doped metal oxide, assuming no electronic traps.

profiles very similar to those shown in Fig. 1 [14], and equilibrium conductivity measurements on thin films of $SrTiO_3$ have also given similar results [15, 16]. These similarities support our conclusion that undoped SBN is behaving like a donor-doped oxide, as will be discussed.

The following discussion will focus on Regions I and II , the regions with log-log slope of $-1/4$ and the plateau, respectively. These regions are typical of donor-doped oxides as shown by the Kröger-Vink diagram of the hypothetical donor-doped oxide MO, Fig. 2 [17]. The abrupt rise in conductivity at lower oxygen activities cannot be accounted for by conventional defect chemistry. We will speculate later on the possible cause of this phenomenon. Data in the region of oxygen activities below the jump do not contain enough information in themselves to support an interpretation.

Qualitative thermoforce measurements were made at 775°C in both Region I {[log $P(O_2)$/atm.] $= -3.1$} and Region II {[log $P(O_2)$/atm.] $= -6.5$}. The results, which can be seen in Fig. 3(a) and (b), were very similar. The linearity shows that the thermoforce is independent of the temperature gradient, and the negative slopes indicate that the conductivity is *n*-type in both regions. This is consistent with donor-doped behavior.

In order to minimize the apparent decomposition of SBN at low oxygen activities, a set of equilibrium conductivity measurements of undoped SBN were made between 625 and 750°C with minimal exposure to the more reducing atmospheres, as shown in Fig. 4. For Region I, an Arrhenius plot of $\sigma T P(O_2)^{1/4}$ was made for log [$P(O_2)$/atm.] values near -3.1, Fig. 5. In Region II an Arrhenius plot of σT was made for values at log [$P(O_2)$/atm.] $= -7.0$, Fig. 6. The resulting activation energies of conduction are 1.81 eV in Region I and 1.63 eV in Region II.

The equilibrium conductivity of SBN acceptor-doped by replacing 1% of the Ta^{+5} with Ti^{+4}, Ti'_{Ta}, is compared with that of undoped SBN in Fig. 7. The level of conductivity has been reduced from that of undoped SBN by a factor of 2–3, but the general shape is unchanged. Thus the added 1% acceptor content has not been sufficient to change the conductivity to an acceptor-doped behavior. This suggests that the undoped SBN already has a donor content of the order of 1–2%.

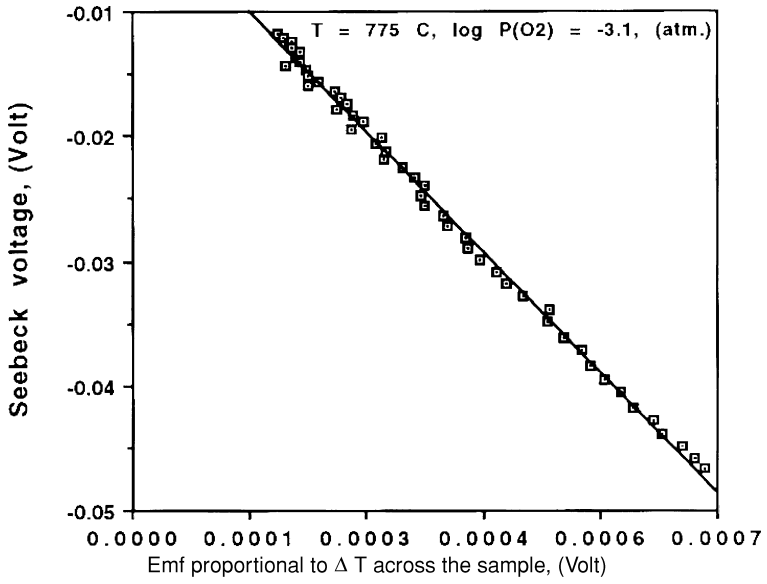

(a)

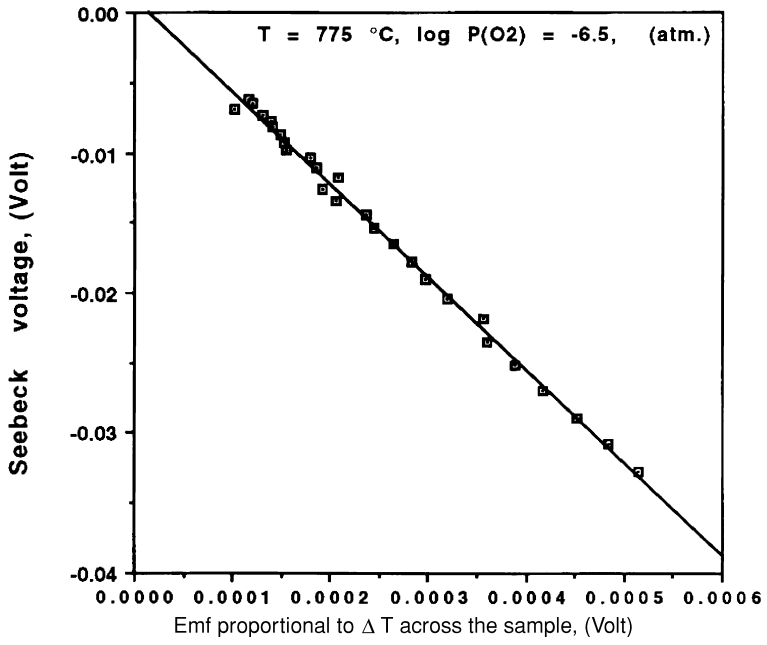

(b)

Fig. 3. (a) and (b) The Seebeck voltage as a function of ΔT for an undoped SBN sample at 775°C and $\log[P(O_2)/\text{atm.}] = -3.1$, and at 775°C and $\log[P(O_2)/\text{atm.}] = -6.5$, respectively.

Discussion

The crystal structures of SBN and SBT were originally considered to be face-centered-orthorhombic with space group Fmmm [10]. More recent studies have determined that the structures are actually A-centered-orthorhombic with space group $A2_1am$ [6, 7]. However, this new assignment preserves the originally accepted two-layered structure, which is formed by alternating fluorite-like $Bi_2O_2^{+2}$ and perovskite-like $SrNb_2O_7^{-2}$

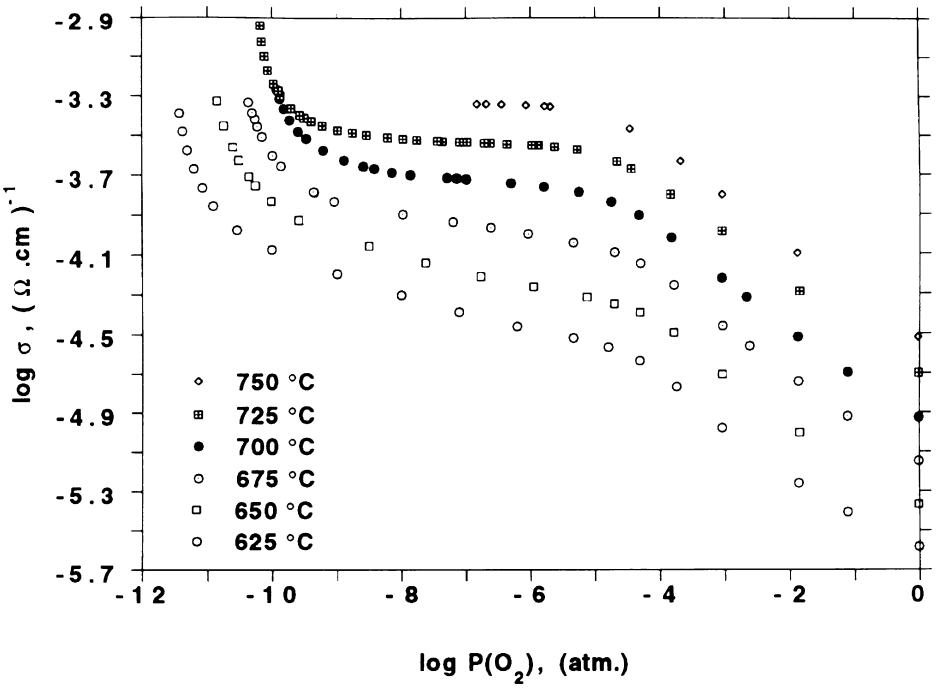

Fig. 4. The partial equilibrium conductivity curves for undoped SBN for values of temperature between 625°C and 750°C at 25°C intervals. The lowermost oxygen activities were avoided in order to increase the life time of the sample.

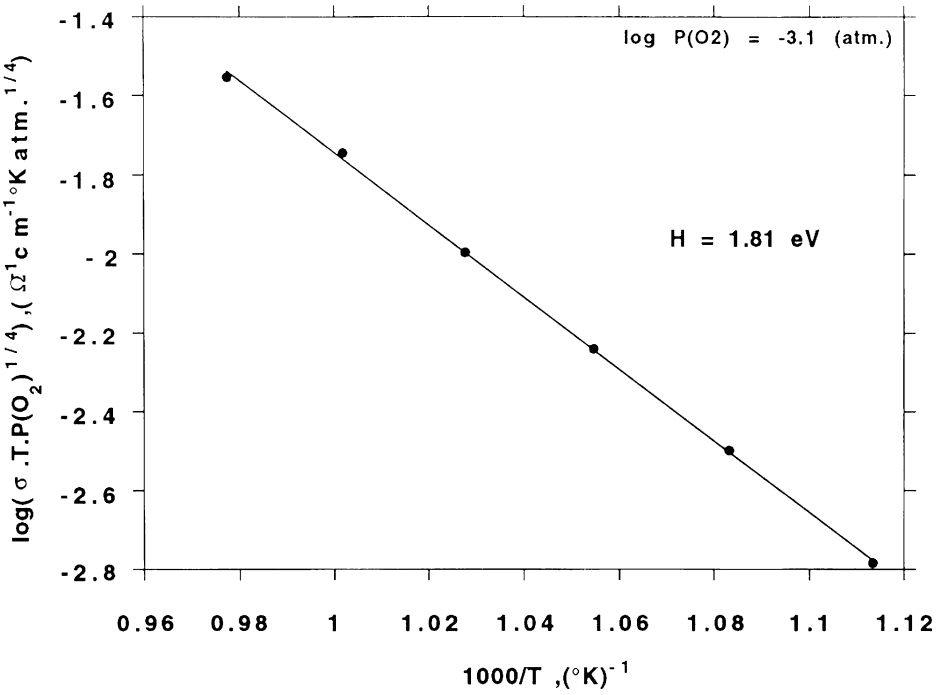

Fig. 5. The Arrhenius plot of $\log[\sigma TP(O_2)^{1/4}/\text{atm.}]$ for the conductivity isotherms of undoped SBN in Fig. 4 at $\log[P(O_2)/\text{atm.}] = -3.1$.

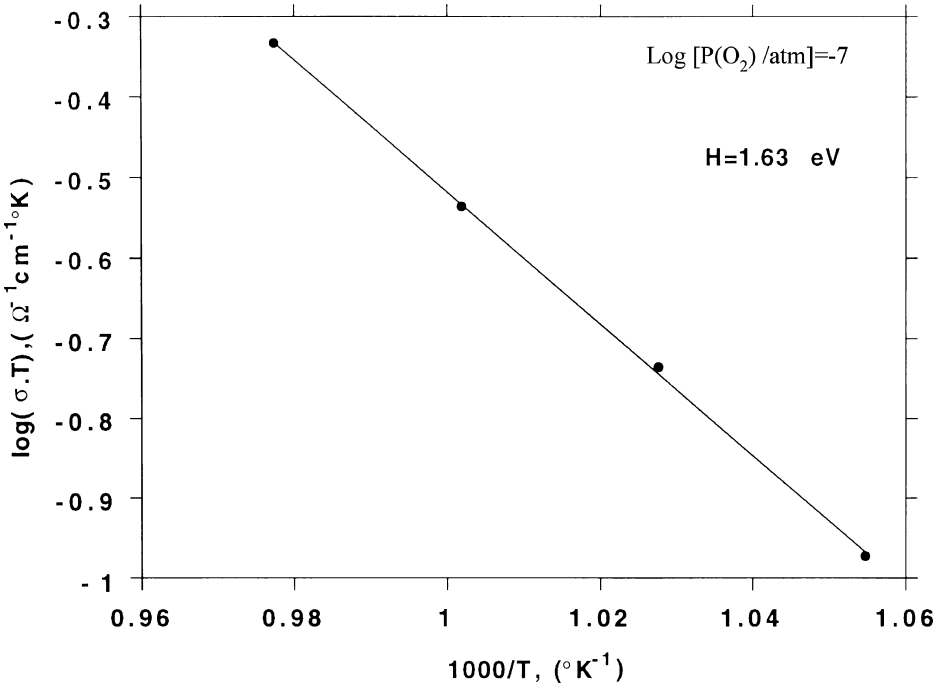

Fig. 6. The Arrhenius plot of $\log[\sigma T/\text{atm.}]$ for the top four conductivity isotherms of undoped SBN in Fig. 4 at $\log[P(O_2)/\text{atm.}] = -7$.

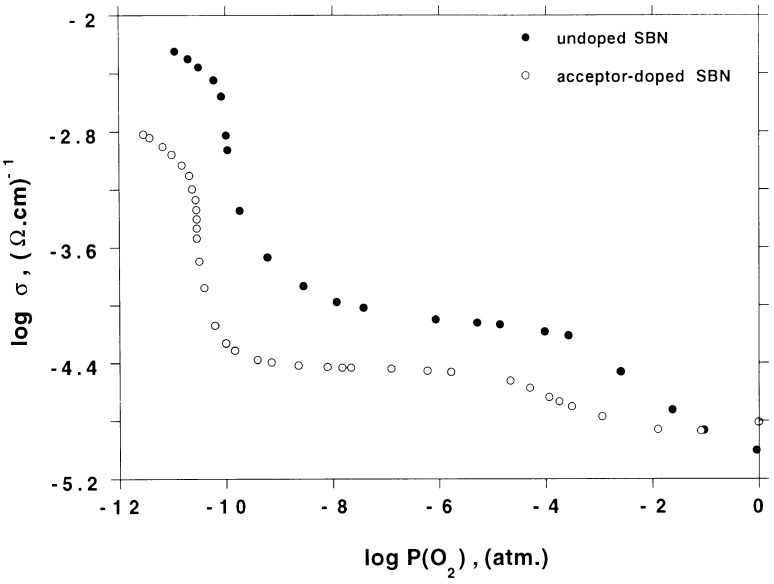

Fig. 7. The equilibrium conductivity of undoped and 1% acceptor-doped ($Ti^{\bullet}_{Ta}$) SBN at 700°C.

layers. The detailed structural studies of both SBN and SBT indicate that there is substantial place exchange between Sr^{+2} and Bi^{+3} in the structures. This exchange amounts to several percent. This results in the presence of Sr'_{Bi} in the Bi-layers, and $Bi^{\bullet}_{Sr}$ in the perovskite layers. Such shuffling of cations within an isotropic structure would be self-compensating without need for the presence of other charge-compensating

defects. However, we have proposed that in these layered structures the self-compensation is not fully effective, and that there is then some charge-compensation on a local basis. As a result, the $Bi_2O_2^{+2}$ layers have a net excess acceptor content that can be compensated by oxygen vacancies ($V_O^{\bullet\bullet}$) or holes ($h^{\bullet}$), while the perovskite layers have a net excess donor content compensated by cation vacancies (V''_{Sr}) or electrons (e'). In randomly oriented polycrystalline samples, the electrical conductivity should be dominated by the better conducting layer. In SBT it was proposed that the observed $P(O_2)$-independent ionic conductivity is due to compensating oxygen vacancies in the Bi-layers. Doping studies indicated that the excess acceptor content, Sr'_{Bi}, in these layers is about 1–2%.

It was previously concluded that the most likely mechanism for the cation place exchange was by exchanging 3 units of SrO for 1 unit of Bi_2O_3 [9]. Thus in the perovskite layer,

$$Bi_2O_3 \xrightarrow{(3SrO)} 2Bi^{\bullet}_{Sr} + 3O_o + V''_{Sr} \qquad (1)$$

while in the Bi layer,

$$3SrO + Bi_{Bi} + 3/2O_o \xrightarrow{(Bi_2O_3)} 3Sr'_{Bi} + 3O_o + 3/2V_o^{\bullet\bullet} + 1/2Bi_2O_3 \qquad (2)$$

We believe that scattered, yellow-colored stains observed on the surface of the samples represent the Bi_2O_3 exsolved by the latter reaction. These stains have a glassy appearance as if they had been melted, and EDS measurements indicate that they are slightly Bi-rich relative to other areas on the surface. Thus the Sr^{+2} in the Bi layers are partially compensated by oxygen vacancies, while the Bi^{+3} in the perovskite layers are partially compensated by cation vacancies or electrons. It was proposed that the equilibrium conductivity of SBT was primarily due to oxygen vacancy conduction in the Bi layers. We now suggest that the equilibrium conductivity of SBN is dominated by conduction by electrons in the perovskite layer. A possible reason for these different behaviors will be discussed later.

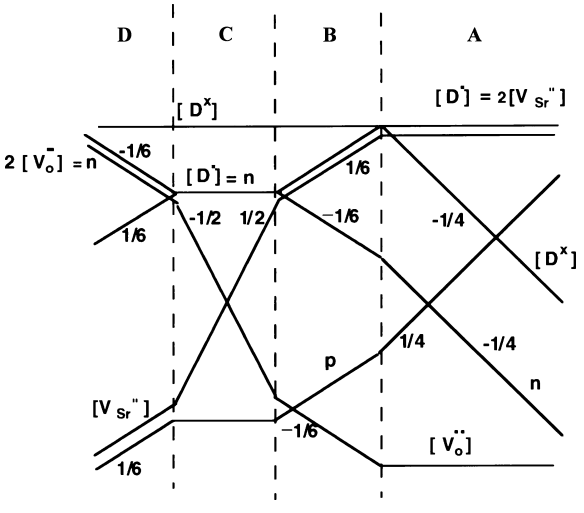

Fig. 8. Equilibrium defect diagram for a donor-doped metal oxide with deep electron traps. The approximate expression for charge neutrality is the same in Regions A and B, $2[V''_{Sr}] = [D^{\bullet}]$.

The equilibrium conductivity of SBN in Regions I and II will now be analyzed in terms of *n*-type conduction in a donor-doped oxide, the perovskite layers in this case. The discussion is also pertinent to the results obtained for highly donor-doped bulk samples of $SrTiO_3$ [13, 14], and suggests that the defect chemistry of thin films of $SrTiO_3$ is dominated by *n*-type conductivity due to an unidentified source of a large concentration of donor-centers [15, 16]. A Kröger-Vink diagram for a generic donor-doped oxide MO is shown in Fig. 2 [17], for the case that trapping of the charge carriers can be neglected. However, the high values obtained for the activation energies of conduction in Regions I and II suggest that the electrons may be deeply trapped so that only a small fraction of them are ionized into a conducting state. The Kröger-Vink diagram for this situation is shown in Fig. 8. There is still a plateau region, Region C, and a region with log-log slope of $-1/4$, Region A, as in the case without trapping, but they are now separated by a region, Region B, with a log-log slope of $-1/6$. We do not see such a distinct region, but it could be obscured in the transition between slopes. It is necessary to derive these slopes in order to judge the viability of the trapping model.

Region A in Fig. 8 corresponds to the case of compensation of the donor centers by an ionic defect, which we will assume to be the strontium vacancy, V''_{Sr}

$$[Bi^{\bullet}_{Sr}] \approx 2[V''_{Sr}] \qquad (3)$$

It is also assumed that most of the electrons are trapped such that

$$[Bi^{\bullet}_{Sr}] > \left[Bi^{x}_{Sr}\right] > n \qquad (4)$$

The reduction reaction can then be viewed as the consumption of Sr vacancies and the creation of electrons,

which are mostly trapped by the donor centers

$$V''_{Sr} + 2Bi^{\bullet}_{Sr} + O_o \leftrightarrow 1/2O_2 + 2Bi^{x}_{Sr} \tag{5}$$

This reaction has the mass-action expression

$$\frac{\left[Bi^{x}_{Sr}\right]^2}{[Bi^{\bullet}_{Sr}]^2[V''_{Sr}]} = K_{red}P(O_2)^{-1/2} \tag{6}$$

There is then an ionization reaction for the trapped electrons

$$Bi^{x}_{Sr} \leftrightarrow Bi^{\bullet}_{Sr} + e' \tag{7}$$

With the mass-action expression

$$\frac{[Bi^{\bullet}_{Sr}]n}{\left[Bi^{x}_{Sr}\right]} = K_D \tag{8}$$

The two equilibrium reactions can be combined to give the reduction reaction to form free electrons, with its corresponding mass-action expression

$$V''_{Sr} + O_o \leftrightarrow 1/2O_2 + 2e' \tag{9}$$

$$\frac{n^2}{\left[V''_{Sr}\right]} = K'_nP(O_2)^{-1/2} \tag{10}$$

In Region A, combination of Eqs. (3) and (10) gives for the free electron concentration

$$n \approx \left(\frac{K'_n[Bi^{\bullet}_{Sr}]}{2}\right)^{1/2} P(O_2)^{-1/4} \tag{11}$$

and for the trapped electron concentration Eqs. (3), (8), and (11) give

$$\left[Bi^{x}_{Sr}\right] \approx \left(\frac{K_{red}}{2}\right)^{1/2} [Bi^{\bullet}_{Sr}]^{3/2}P(O_2)^{-1/4} \tag{12}$$

The predicted log-log slope of $-1/4$ corresponds to the observed dependence of the conductivities at the highest oxygen activities. The trapped electron concentration runs parallel to the free electron concentration, but at a higher level.

In Region B, the trapped electron concentration has reached the level of the total donor concentration and almost all donors have trapped an electron to become a neutral donor species. Charge neutrality is still controlled by Eq. (3), and there is the added condition that the neutral donor concentration is invariant with oxygen activity

$$\left[Bi^{x}_{Sr}\right] \approx c \tag{13}$$

Combination of Eqs. (3), (6), and (13) gives

$$2[V''_{Sr}] \approx [Bi^{\bullet}_{Sr}] \approx \left(\frac{2c^2}{K_{red}}\right)^{1/3} P(O_2)^{1/6} \tag{14}$$

and substituting this into Eq. (8) gives

$$n \approx c^{1/3}K_D\left(\frac{K_{red}}{2}\right)^{1/3} P(O_2)^{-1/6} \tag{15}$$

$[Bi^{\bullet}_{Sr}]$ and n now converge to a new condition of charge neutrality in Region C, the plateau region.

$$n \approx [Bi^{\bullet}_{Sr}] \tag{16}$$

From Eqs. (6), (8), (13), and (16), the cation vacancy concentration is given by

$$[V''_{Sr}] \approx \frac{cP(O_2)^{1/2}}{K_{red}K_D} \tag{17}$$

The oxygen vacancy concentrations shown in Fig. 8 assume that there is some kind of a Schottky-like relationship between the cation and anion vacancies. This is obviously too simplistic for such a complex compound. This point has been discussed in detail by Moos and Härdtl in their extensive study of donor-doped $SrTiO_3$ [18]. For the present model, the oxygen vacancy concentration rises with reduction to the level of $[D^{\bullet}]$ and displaces it from the approximation to charge neutrality to give

$$n \approx 2[V^{\bullet\bullet}_o] \tag{18}$$

The reduction reaction and its mass-action expression

$$O_o \leftrightarrow 1/2O_2 + V^{\bullet\bullet}_o + 2e' \tag{19}$$

$$[V^{\bullet\bullet}_o]n^2 = K_nP(O_2)^{-1/2} \tag{20}$$

now dominate the behavior in Region D. Combination of Eqs. (18) and (20) give the familiar relatonship

$$n \approx (2K_n)^{1/3}P(O_2)^{-1/6} \tag{21}$$

It will be shown in a later publication that for SBN, the log-log slope in Region D is indeed consistent with

the predicted value of $-1/6$, but it is displaced upward from the ideal case shown in Fig. 8 by the vertical jump in conductivity.

In Region B, $[Bi^{\bullet}_{Sr}]$ and n converge with reduction with log-log slopes of $+1/6$ and $-1/6$, respectively. It is apparent that the width of Region B depends on the separation between n and $[Bi^{x}_{Sr}]$ in Region A. From Eq. (8) their ratio is given by

$$\frac{n}{[Bi^{x}_{Sr}]} = \frac{K_D}{[Bi^{\bullet}_{Sr}]} \tag{22}$$

where $[Bi^{\bullet}_{Sr}]$ is fixed and K_D is largely determined by the ionization energy for the trapped electrons. If all of the observed activation energy of conductivity of about 1.6 eV were due to the ionization energy, and if $[Bi^{\bullet}_{Sr}]$ is taken to be of the order of 0.01, then the ratio $n/[Bi^{x}_{Sr}]$ at 700°C is approximately 10^{-6}. This would require that Region B have a width of 18 orders of magnitude of oxygen activity. That is obviously not the case. The data indicate that this width can be no more than a very few orders of magnitude so that the $-1/6$ slope does not emerge clearly from the transition between regions. Thus very little of the observed activation energy of conductivity can be attributed to the ionization energy for trapped electrons. If the electron concentration in Region II is not thermally activated, then the only alternative would seem to be that the electron mobility is very highly activated.

Our conclusion then is that the equilibrium conductivity of undoped SBN is an n-type conductivity due to the donor centers, $Bi^{\bullet}_{Sr}$, in the perovskite layers, and that the electrons are mostly not trapped and have highly activated mobilities. This means that Region B in Fig. 8 has negligible width, and that the behavior of undoped SBN is better represented by Fig. 2. According to this model, the electron and donor concentrations are equal in the plateau region, Region II, and the electron mobility can thus be calculated from the donor concentration and the conductivity. The donor concentration appears to be about 1%, or 1.5×10^{20} cm^{-3}, so the mobility at 750° is of the order of 10^{-5} cm^2/v · sec with an activation energy of 1.6 eV. Note that this interpretation implies that SBN is a conventional insulator with a significant band gap. Indeed a band gap of 4.2 eV has been measured in SBT by UV photoemission spectroscopy [19].

It is seen in Figs. 4 and 7 that for undoped SBN at the lower temperatures, the data points taken at $P(O_2) = 1$ atm. are higher than would be expected from an extrapolation of the log-log slope of $-1/4$. In other words the slope is becoming more shallow. In fact, for the 1% acceptor-doped sample in Fig. 7, a shallow minimum appears and the slope changes to positive values as 1 atm. is approached. The minimum corresponds approximately to the condition $n = p$ shown in Fig. 2. It is indeed expected to move to lower values of $P(O_2)$ with increasing acceptor content. The shallow shape of the minima may well be due to the $P(O_2)$-independent, parallel ionic conduction in the Bi-layers.

In Region I the electrons are formed by the reduction reaction, Eq. (9), and their concentration is given by Eq. (11). The concentration is proportional to $K_n'^{1/2}$, and given the usual form for a mass-action constant, $K = K' \exp(-H/kT)$, is thus proportional to $\exp(H_n'/2kT)$, where H_n' is the enthalpy of Eq. (9). The conductivity should then be proportional to $\exp(H_n'/2 + H_m)/kT$, where H_m is the assumed activation energy for the electron mobility. In the plateau region, the electron concentration is fixed by the donor concentration, so that the conductivity should be proportional only to $\exp(H_m/kT)$. The measured value for H_m is 1.63 eV, while that for $H_n'/2 + H_m$ is 1.81 eV. From this it is seen that $H_n' = 0.36$ eV, a rather small number. It is possible to measure H_n' directly, by means of a technique previously described [11]. Rearrangement of Eq. (11) gives

$$P(O_2) \approx \left(\frac{[Bi_{Sr}]^2}{4n^4}\right) K_n'^2 \tag{23}$$

Thus the measurement of the equilibrium oxygen activity as a function of temperature will give the enthalpy of the reduction reaction if the expression in parentheses can be kept constant. We call this a constant defect measurement. The experiment is designed so that the alumina measurement cell is nearly filled with the sample; the goal is to have the maximum mass of sample in equilibrium with a minimum volume of gas phase. One end of the cell is hermetically sealed with an alumina disk by means of a glass ring that softens in the experimental temperature range. The other end is similarly sealed with a doped zirconia disk that has been electroded with platinum on both sides. A platinum wire is brought out from the inner electrode through the softened glass gasket. After the desired oxygen activity has been established inside the cell, the cell is sealed by exerting pressure on the softened glass rings. One can then measure the emf of the oxygen concentration cell developed across the electrolyte disk

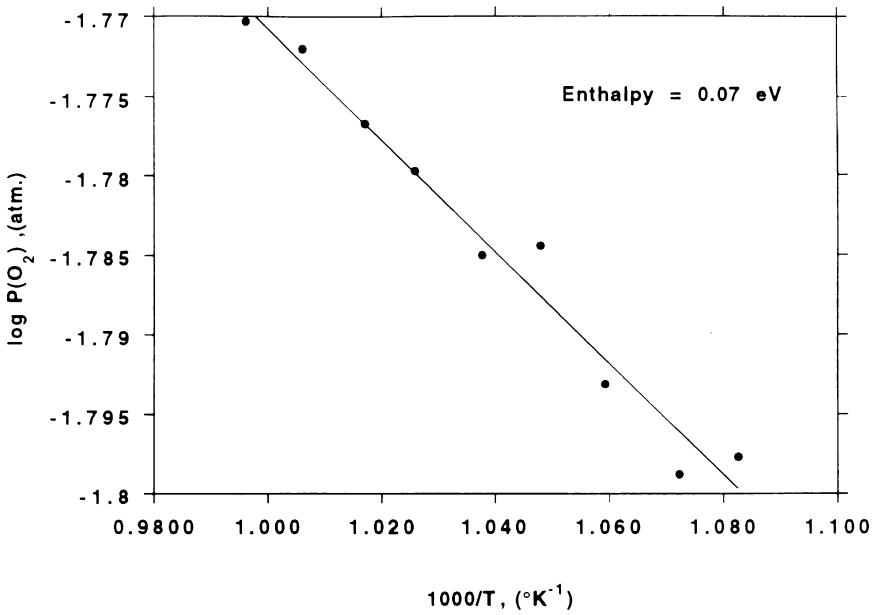

Fig. 9. The Arrhenius plot of log[$P(O_2)$/atm.] for a constant composition oxygen activity measurement for undoped SBN in a sealed cell.

by the different activities inside and outside the cell. Thus the oxygen activity in equilibrium with the sample can be measured over some range of temperature. With the large sample mass, and small gas volume, the amount of oxygen that must enter or leave the sample to create the new equilibrium activity in the gas phase is small compared to the defect concentration, thus fulfilling the necessary conditions to obtain the enthalpy of reduction. Such an Arrhenius plot is shown in Fig. 9 for activities corresponding to Region I. The enthalpy of reduction is determined to be 0.07 eV, even smaller than the value derived above. Examination of Fig. 4 shows that the plateau region is never actually horizontal at the lower temperatures, and there is thus the potential for uncertainty in the precise value of H_m. Thus the agreement between the two determinations is satisfactory within the accuracy of the data. In any case, the enthalpy of reduction is quite small, and this is consistent with the similarity of the temperature dependencies in Regions I and II.

The Difference Between SBT and SBN

Why do these very similar, isostructural compounds behave so differently? In SBT we see primarily ionic conductivity that we attribute to oxygen vacancy conduction in the Bi-layer due to the acceptor center content. In SBN we see n-type electronic conductivity that we attribute to the donor center content of the perovskite layers. The level of ionic conductivity should be largely determined by the acceptor concentration in the Bi layers, which seems to be about 1–2%. The level of electronic conductivity is set by the general magnitude of electronic disorder, as indicated by the band gap. As seen in Fig. 2, the electronic disorder can be viewed as starting at the point where $n = p$, where both are proportional to $\exp(-E_g^o/2kT)$. The n-type conductivity increases with decreasing $P(O_2)$ below the location of $n = p$, while p-type conductivity increases with increasing $P(O_2)$ above the location of $n = p$. Thus the smaller the band gap, the higher the overall level of electronic conductivity. The major chemical difference between Nb^{+5} and Ta^{+5} is that the former is more easily reduced, and there is much more chemistry of the lower oxidation states of Nb. Compounds of Nb^{+5} are then expected to have smaller band gaps than their Ta^{+5} analogs. This explains why in SBN the electronic conductivity in the perovskite layers overpowers the ionic conduction in the Bi layers.

The equilibrium conductivity of $SrBi_2NbTaO_9$, SBNT, is shown in Fig. 10. The behavior is qualitatively like that of SBN, but at a lower conductivity

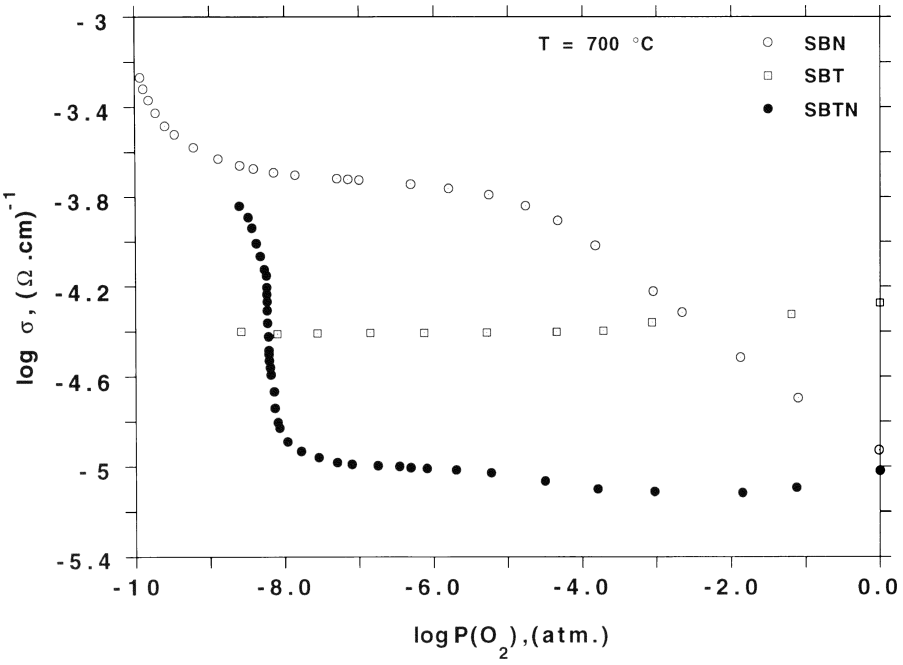

Fig. 10. The equilibrium conductivity of SBNT, SBN and SBT at 700°C.

level. The band gap of SBNT would be expected to lie between those of SBN and SBT. Thus one expects to see a lower level of *n*-type conductivity in SBNT than in SBN, and that is indeed the case.

The Rate of Equilibration

The equilibration rates of donor-doped $BaTiO_3$ and $SrTiO_3$ are notoriously slow [13, 14, 19]. This is because the oxygen vacancy concentration, on which the equilibration process depends, has been reduced to very low levels. Indeed in both the work on Nb-doped [13] and on La-doped [14] $SrTiO_3$, the samples were deliberately made very porous to reduce the equilibration times by three orders of magnitude at the measurement temperature range of 725–1000°C. Yet in SBN we obtained quite reasonable equilibration times in our sintered samples at 650 to 775°C. This can be explained by the structure and self-doping of SBN. The donor-doped perovskite layers are sandwiched between acceptor-doped Bi layers in which oxygen is very mobile. These layers serve as pipelines for the oxygen, which, then has to diffuse only a few angstroms into the donor-doped perovskite layers.

The Jump in Conductivity

The most striking aspect of the equilibrium conductivity of SBN, and of recent studies of donor-doped $SrTiO_3$ [13, 14] and thin film $SrTiO_3$ and $(Ba_{1-x}Sr_x)TiO_3$ [15, 16], is the abrupt jump in conductivity, Region II′, between Regions II and III. Such a sharp rise in conductivity cannot be accommodated by conventional defect chemistry. For $P(O_2)$ values lower than that at the jump, the conductivity reverts to more normal behavior, and it will be shown in a subsequent publication that it is best described as having a log-log slope of $-1/6$, and this has been readily observed in the thin films of the much more stable compound $SrTiO_3$ [16]. A log-log slope of $-1/6$ is characteristic of highly reduced behavior, Eq. (21). We have concluded that the electrons in SBN are strongly localized, and conduct by a highly activated mobility with an activation energy of about 1.6 eV. From Fig. 1 it is seen that the temperature dependence in Region III, below the jump in conductivity, is much less than in the plateau region, Region II. In the latter it was concluded that the temperature dependence was due to the activation energy of the electron mobility. This suggests that the conductivity jump represents the partial release of a highly

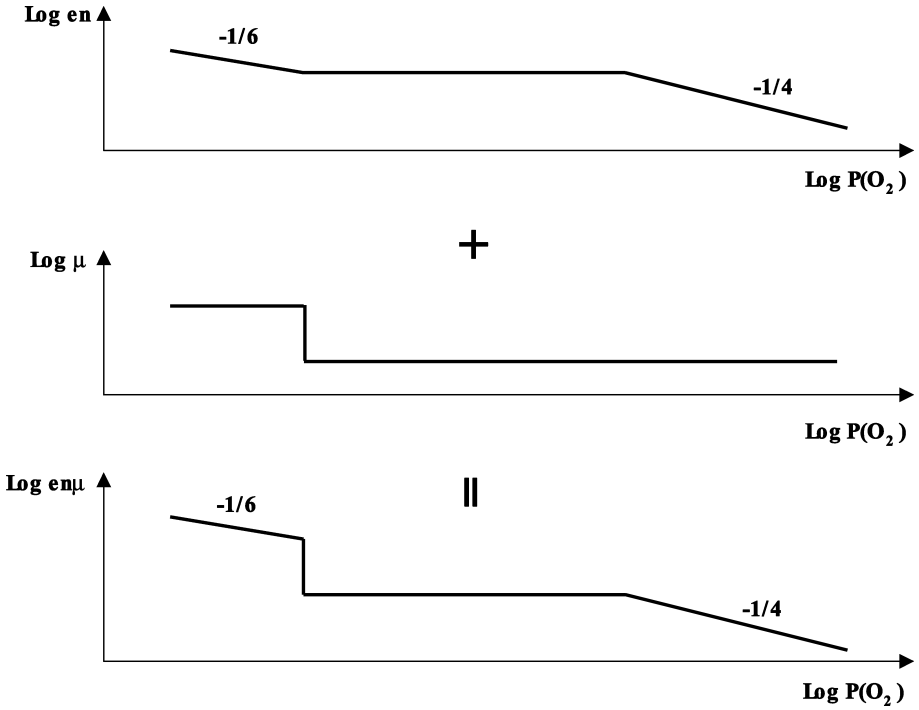

Fig. 11. The cartoon for the proposed model for the conductivity jump.

restricted mobility. In fact, a decrease in the activation energy of mobility from 1.6 to 1.4 eV is enough to account for the jump in conductivity. Below the jump, the behavior reverts to normal and the temperature dependence should be related to $\exp(\Delta H_n/3 + H'_m)/kT)$, where ΔH_n is the enthalpy of the intrinsic reduction reaction, Eq. (19), and H'_m is a reduced activation energy of mobility. In this picture, the equilibrium conductivity of SBN is that of a conventional donor-doped oxide, except that the electron mobility in Region III is much greater than in Regions I and II. In the latter, it was concluded that the temperature dependence was due to the activation energy of the electron mobility. We suggest that the jump results from a partial release from this restricted mobility, and that this release occurs close to where the oxygen vacancy concentration becomes comparable with the donor concentration. The relatively slow climb of the conductivity, which goes on for about 8 h until it saturates, suggests a process involving an atomic rearrangement. This does not appear to be due to a structural change, since the X-ray diffraction patterns for samples quenched from above and below the conductivity jump are the same. Thus any such rearrangement must be highly localized. According to this model, which is given schematically in Fig. 11, the behavior of the n-type conductivity in SBN is equivalent to that of any simple, donor-doped oxide, except that the electron mobility in Region III is much greater than in Regions I and II. The logarithm of conductivity, $\log \sigma$, is equal to $\log en\mu$, where, the electronic charge, electron concentration, and electron mobility, are denoted as e, n, and μ, respectively. Since it is possible to write the expression, $\log \sigma = \log en + \log \mu$, a change in the mobility will be reflected as a shift in the value of the logarithm of the conductivity. Figure 11 depicts this model in a schematic way.

The Presence of Metallic Bi on the Surface

The presence of metallic Bi on the surface of SBT, as determined by XPS, has been reported by Ono et al. [21, 22]. We reported previously that while an XPS signal for metallic Bi was present on original surfaces of SBT, no such signal was observed for a fresh fracture surface created in the XPS apparatus [9]. It was concluded that the metallic Bi was created by the highly reducing atmosphere and the electron flood gun, in the

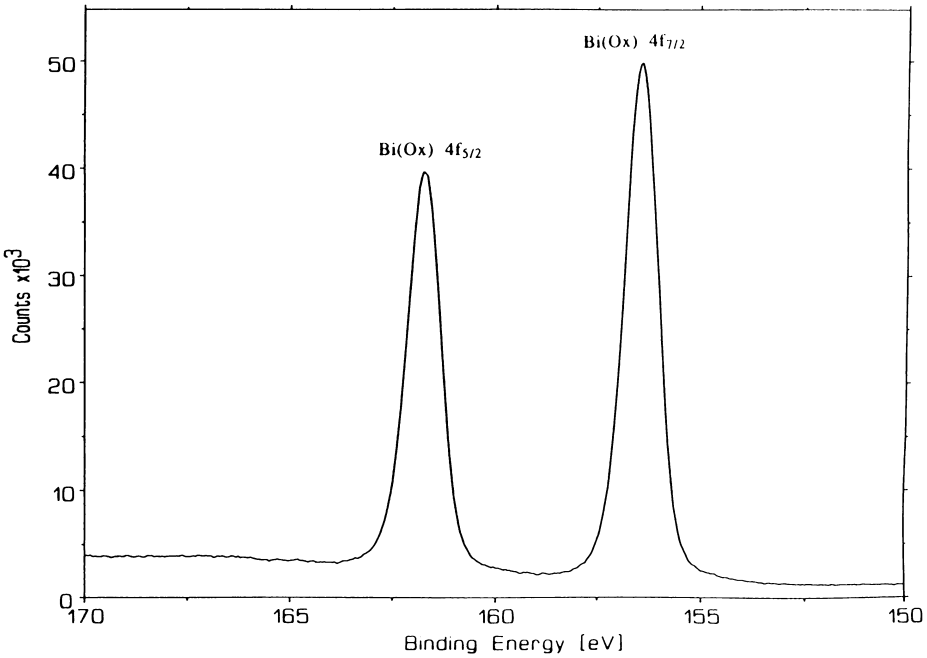

Fig. 12. Core level XPS signal from Bi^{3+} 4f (ox) on a freshly formed fracture surface of SBN.

XPS apparatus, and was not present on the samples equilibrated in air or oxygen. That is consistent with the thermodynamic instability of Bi in oxidizing atmospheres. We have now obtained similar results with SBN, in Figs. 12 and 13, with the added observation that while no signal for metallic Bi was observed on a fresh fracture surface, the signal did appear after the fracture surface had been exposed overnight to the XPS atmosphere.

Ferroelectric Fatigue

We have attributed the resistance to ferroelectric fatigue in SBT to the absence of mobile charge carriers in the perovskite layer, which is the location of the ferroelectric response in SBT and SBN [9]. There are no carriers sufficiently mobile to migrate to domain boundaries and pin their motion. This concept is strongly supported by the properties of SBN reported here. The electron mobility in the perovskite layers is very low and highly activated with an activation energy of 1.6 eV. This means that they will be extremely immobile at component use temperatures. The electrons in the perovskite layers of SBT behave similarly, as will be shown in a subsequent publication.

Summary

The defect chemistry of SBN and SBT is dominated by cation place exchange between Sr^{+2} and Bi^{+3}. In these layered structures this place exchange is not fully self-compensating, as would be expected in an isotropic structure. Thus the Bi-layer has an excess acceptor content of about 1–2%, due to Sr'_{Bi}, which is compensated by oxygen vacancies. The perovskite layer has an excess donor content of about 1–2%, due to $Bi^{\cdot}_{Sr}$, which is compensated by cation vacancies or electrons, depending on the oxygen activity. In SBT, the equilibrium conductivity is dominated by ionic conduction due to the oxygen vacancies in the Bi-layer. In SBN, the conduction is *n*-type due to electrons in the perovskite layer. In Regions I and II, the behavior is conventional except that the electron mobility is small, of the order of 10^{-5} $cm^2/v \cdot sec$ at 750°C, and has an activation energy of 1.6 eV. Below Region II, there is an abrupt jump in the conductivity with further reduction, and this cannot be explained by conventional defect chemistry. It is suggested that it results from a partial release from

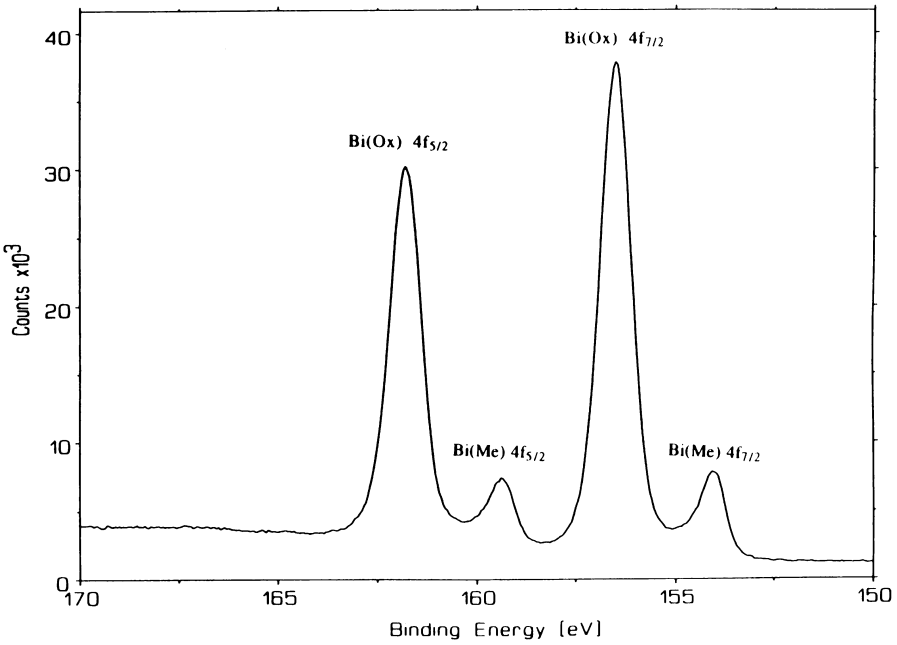

Fig. 13. Core level XPS signal from Bi^{3+} 4f (ox) and metallic Bi 4f (me) states from the fracture surface of Fig. 13, after it was exposed overnight to ultra-high vacuum, Al Kα, and 5 eV electron flood gun.

the very low electron mobilities that prevail at higher oxygen activities. Below the jump it appears that the behavior reverts to that of a normal, highly reduced transition metal oxide with a typical electron mobility. The strikingly different behavior of SBT and SBN is attributed to the expected lower band gap in SBN. This is anticipated because of the greater reducibility of Nb^{+5} compared with Ta^{+5}. The band gap sets the scale of the electronic contribution to the equilibrium conductivity, and the concentrations of electrons in the perovskite layers of SBN are enough to dominate the ionic conduction in the Bi-layers. The unusually rapid equilibration of donor-doped behavior in SBN is attributed to the high mobility of oxygen in the acceptor-doped Bi-layers. These serve as rapid pipelines for oxygen throughout the structure, and the donor-doped equilibration depends only on diffusion into the perovskite layers perpendicular to the plane of the layers.

Acknowledgment

The authors appreciate the partial support of this project by the Division of Materials Research of the National Science Foundation.

References

1. C.A. Paz de Araujo, J.D. Cuchiaro, L.D. McMillan, M.C. Scott, and J.F. Scott, *Nature (London)*, **374**, 627 (1995).
2. W.L. Warren, D. Dimos, B.A. Tuttle, and D.M. Smyth, *J. Am. Ceram. Soc.*, **77**, 2753 (1994).
3. R. Waser, T. Baiatu, and K.-H. Härdtl, *J. Am. Ceram. Soc.*, **73**, 1645 (1994).
4. H.M. Duiker, P.D. Beale, J.F. Scott, C.A. Paz de Araujo, B.M. Melnick, J.D. Chuciaro, and L.D. McMillan, *J. Appl. Phys.*, **68**, 5783 (1990).
5. W.L. Warren, B.A. Tuttle, and D. Dimos, *Appl. Phys. Lett.*, **67**, 1426 (1995).
6. A.D. Rae, J.G. Thompson, and R.I. Withers, *Acta Crystallogr., Sect. B*, **48**, 418 (1992).
7. S.M. Blake, M.J. Falconer, M. McCreedy, and P. Lightfoot, *J. Mater. Chem.*, **7**, 1609 (1997).
8. A.C. Palanduz and D.M. Smyth, *J. Euro. Ceram. Soc.*, **19**, 731 (1999).
9. A.C. Palanduz and D.M. Smyth, *J. Electroceram.*, **5**, 21 (2000).
10. E.C. Subbarao, *J. Am. Ceram. Soc.*, **45**, 166 (1962).
11. M.V. Raymond and D.M. Smyth, *Ferroelectrics*, **144**, 129 (1993).
12. P.C. Eklund and A.K. Mabatah, *Ref. Sci. Instrum*, **48**, 775 (1977).
13. A.A.L. Ferreira, J.C.C. Abrantes, J.A. Labrincha, and J.R. Frade, *J. Euro. Ceram. Soc.*, **19**, 773 (1999).
14. Unpublished results of A.C. Palanduz, W. Menesklou, and H.L. Tuller on La-doped $SrTiO_3$.

15. C. Ohly, S. Hoffmann-Eifert, K. Szot, and R. Waser, *J. Euro. Ceram. Soc.*, **21**, 1673 (2001).
16. C. Ohly, S. Hoffmann-Eifert, K. Szot, and R. Waser, *Integrated Ferroelectrics*, **38**, 229 (2001).
17. D.M. Smyth, *Prog. Solid State Chem.*, **15**, 145 (1984).
18. R. Moos and K.H. Härdtl, *J. Am. Ceram. Soc*, **78**, 2569 (1995).
19. A.J. Hartmann, R.N. Lamb, J.F. Scott, and C.D. Gutleben, *Integrated Ferroelectrics*, **18**, 101 (1997).
20. N.-H. Chan and D.M. Smyth, *J. Am. Ceram. Soc.*, **67**, 285 (1984).
21. S. Ono, A. Sakakibara, T. Seki, T. Osaka, I. Koiwa, J. Mita, T. Iwabuchi, and K. Asami, *J. Electrochem. Soc.*, **144**, L185 (1997).
22. S. Ono, A. Sakakibara, T. Osaka, I. Koiwa, J. Mita, and K. Asami, *J. Electrochem. Soc.*, **146**, 685 (1999).